A global probabilistic study of the Ocean Heat Content low-frequency variability: atmospheric forcing versus oceanic chaos

Guillaume Sérazin[1,2,3], Alexandre Jaymond[1,2], Stéphanie Leroux[1,2], Thierry Penduff[1,2], Bernard Barnier[1,2], Jean-Marc Molines[1,2], Laurent Bessières[3], Laurent Terray[3], William Llovel[3]

Contents of this file

1. Figures S1 to S5
2. Table S1

Introduction

These supporting information provide additional figures that complement the main article. Table S1 gives the coordinates of the region of studies where OHC is inte-

[1]CNRS, LGGE, F-38041 Grenoble, France.

[2]Univ. Grenoble Alpes, LGGE, F-38041 Grenoble, France.

[3]CNRS/CERFACS, CECI UMR5318, Toulouse, France

grated.Figure S1 is used to illustrate the spread induced by chaotic intrinsic oceanic variability (IOV) on the ocean heat content (OHC) at interannual-to-decadal timescales in the South Atlantic (SA). Maps of the estimated model drift are given in Figure S2 to complement the methodological section 2.4 on the estimate of 1980-2010 regional trends. Maps of intrinsic and forced interannual-to-decadal OHC standard deviations are given in Figure S3 and S4 to complement section 4 and Figure 1 of the main article. Figure S5 shows the same result as Figure 1 but for all spatial scales and is used in section 5 to discuss the potential uncertainty induced by chaotic IOV on in-situ oceanic measurements.

Table S1. Coordinates and name of the regions shown in the bottom map of Figure 1 in the article. The OHC is integrated over these regions for each layer and the results are shown in Figure 2 for interannual-to-decadal variability (Signal-to-noise ratio) and multidecadal variability (31-year trends).

Region	Key	Longitude	Latitude
Indian Antarctic Circumpolar Current	IACC	20°E–169°E	59°S–35°S
Gulf Stream	GS	80°W–30°W	30°N–49°N
Global Ocean	GLO	180°W–180°E	77°S–89°N
Kuroshio	KUR	128°E–165°E	25°N–49°N
Gulf of Alaska	ALA	159°W–130°W	48°N–64°N
Agulhas Current	AGU	10°W–49°E	54°S–24°N
North Pacific Subtropical Gyre	NPSG	180°W–180°E	10°N–35°N
North Altantic Subtropical Gyre	NASG	75°W–20°W	10°N–29°N
Pacifica Antarctic Circumpolar Current	PACC	179°W–180°E	74°S–45°S
South Atlantic Ocean	SA	60°W–19°E	64°S–10°S
South Pacific Subtropical Gyre	SPSG	170°W–80°W	34°S–10°S
Gulf of Mexico	MEX	98°W–82°W	18°N–29°N
Zapiola Anticyclone (Malvinas and Brazil currents)	ZAP	60°W–25°W	54°S–35°S

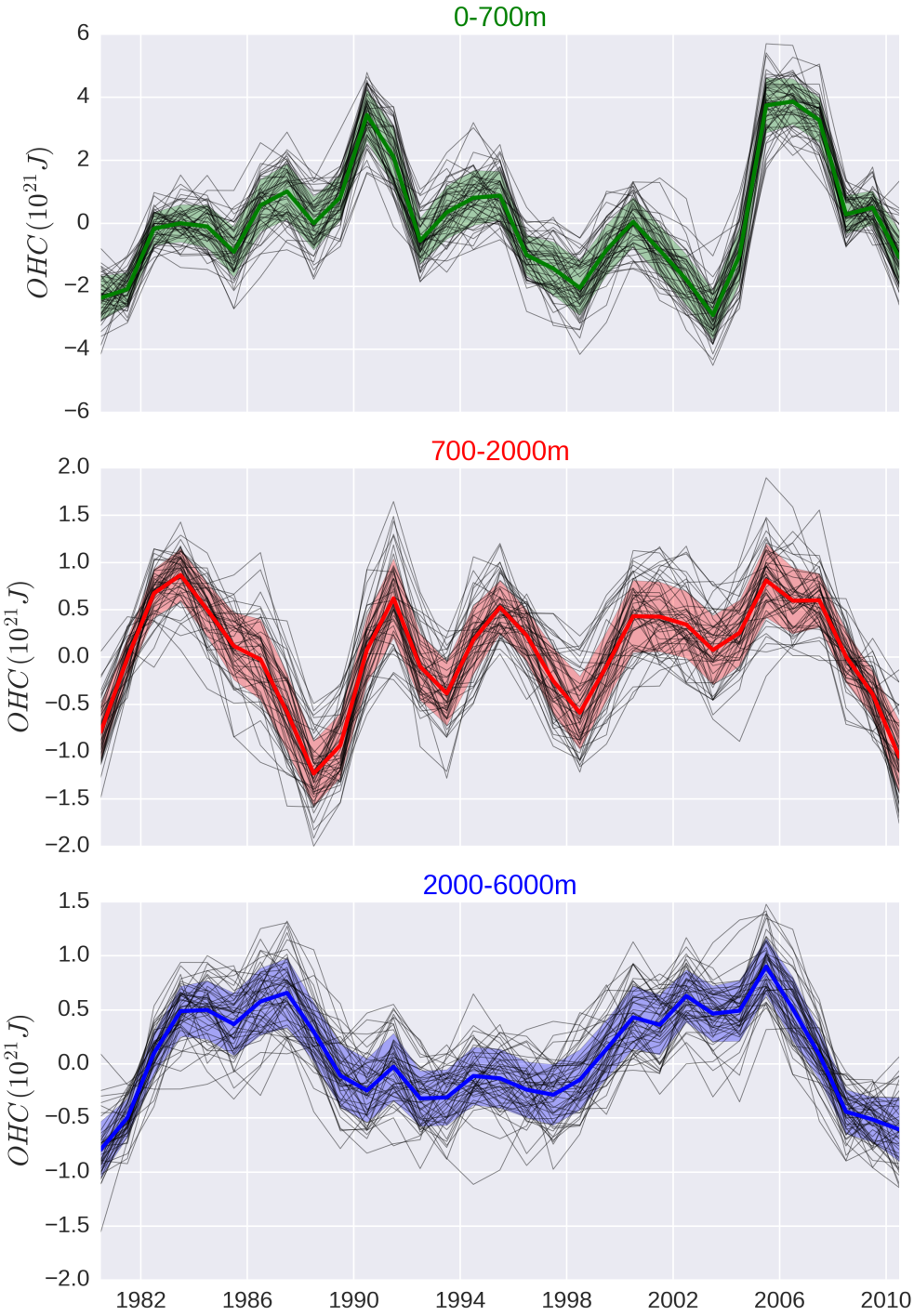

Figure S1. 50 realizations (black curves) of the detrended OHC integrated over the South Atlantic for layers 0-700m (top, green), 700-2000m (middle, red) and 2000-6000m (bottom, blue). The thick curves correspond to the ensemble mean OHC computed from the 50 members ; color shading shows ± one standard deviation around the ensemble mean OHC.

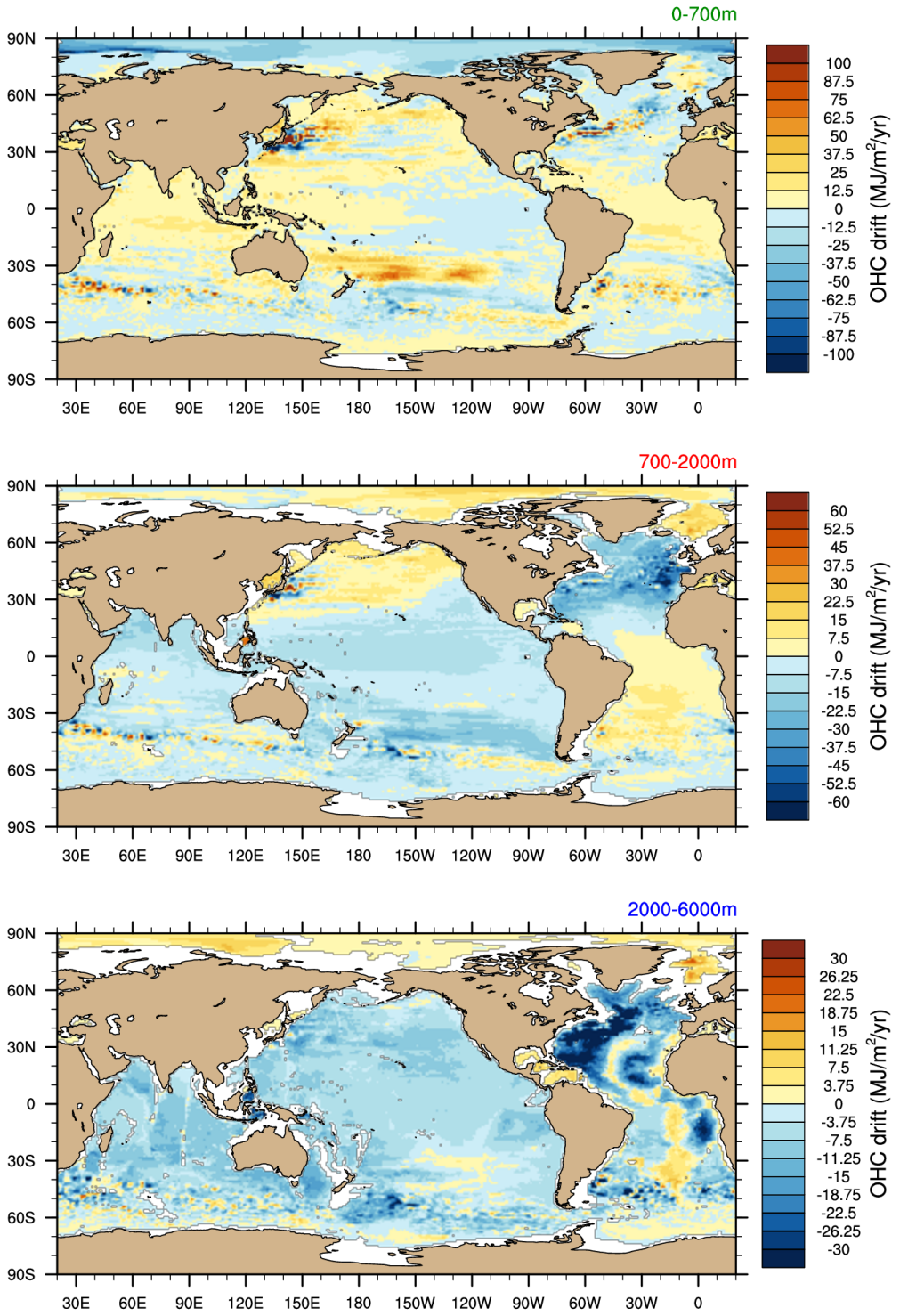

Figure S2. Spurious trend of the regional OHC induced by the model drift and estimated from the climatological simulation over the period 1980-2010 in layers 0-700m (top), 700-2000m (middle) and 2000-6000m (bottom). These spurious trends are removed from the raw OHC trends estimated from each ensemble member to produce Fig. 3

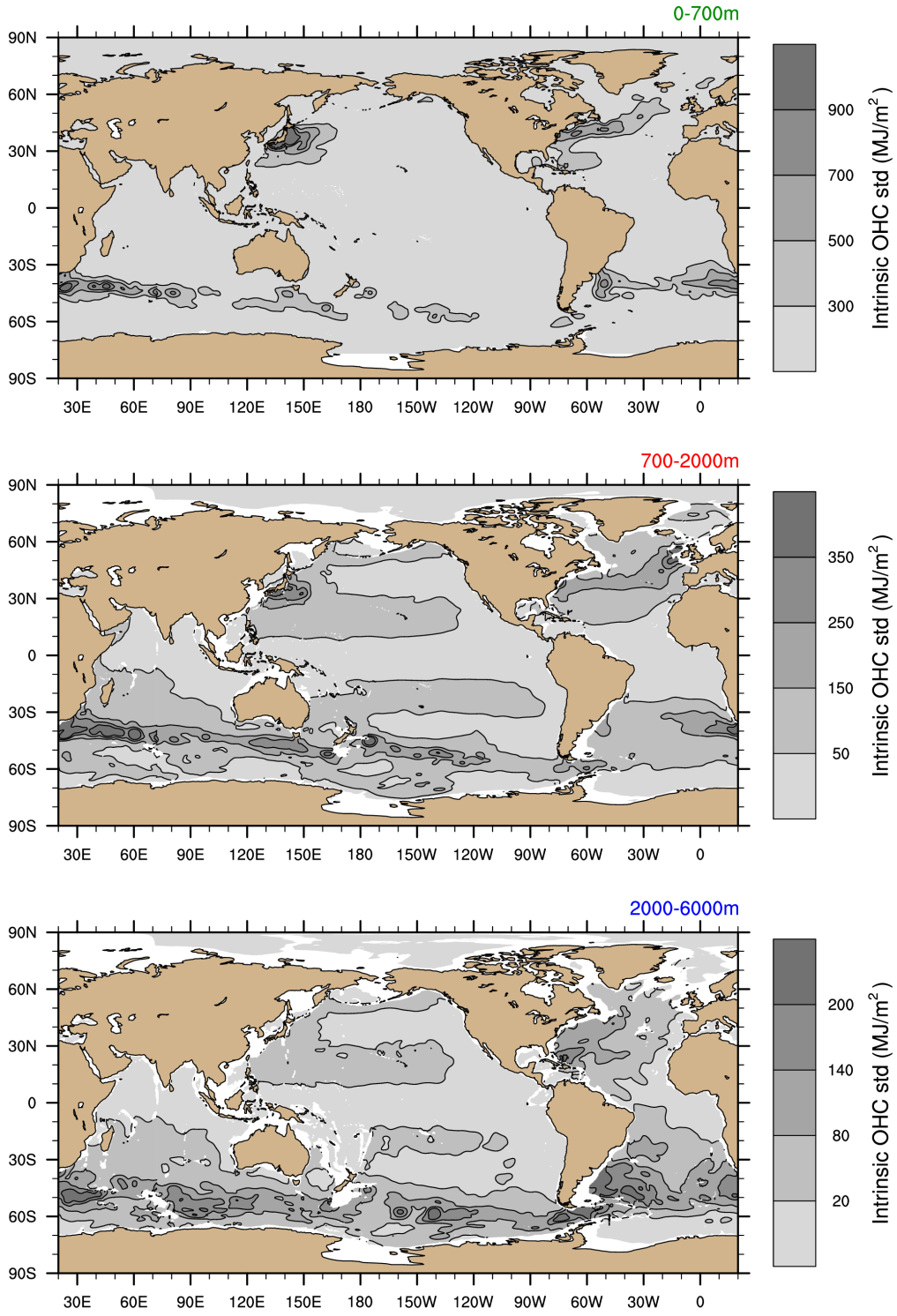

Figure S3. Chaotic intrinsic interannual-to-decadal OHC standard deviation (std, gray shading) at scales larger than 10° x 10°, shown in layers 0-700m (top), 700-2000m (middle) and 2000-6000m (bottom).

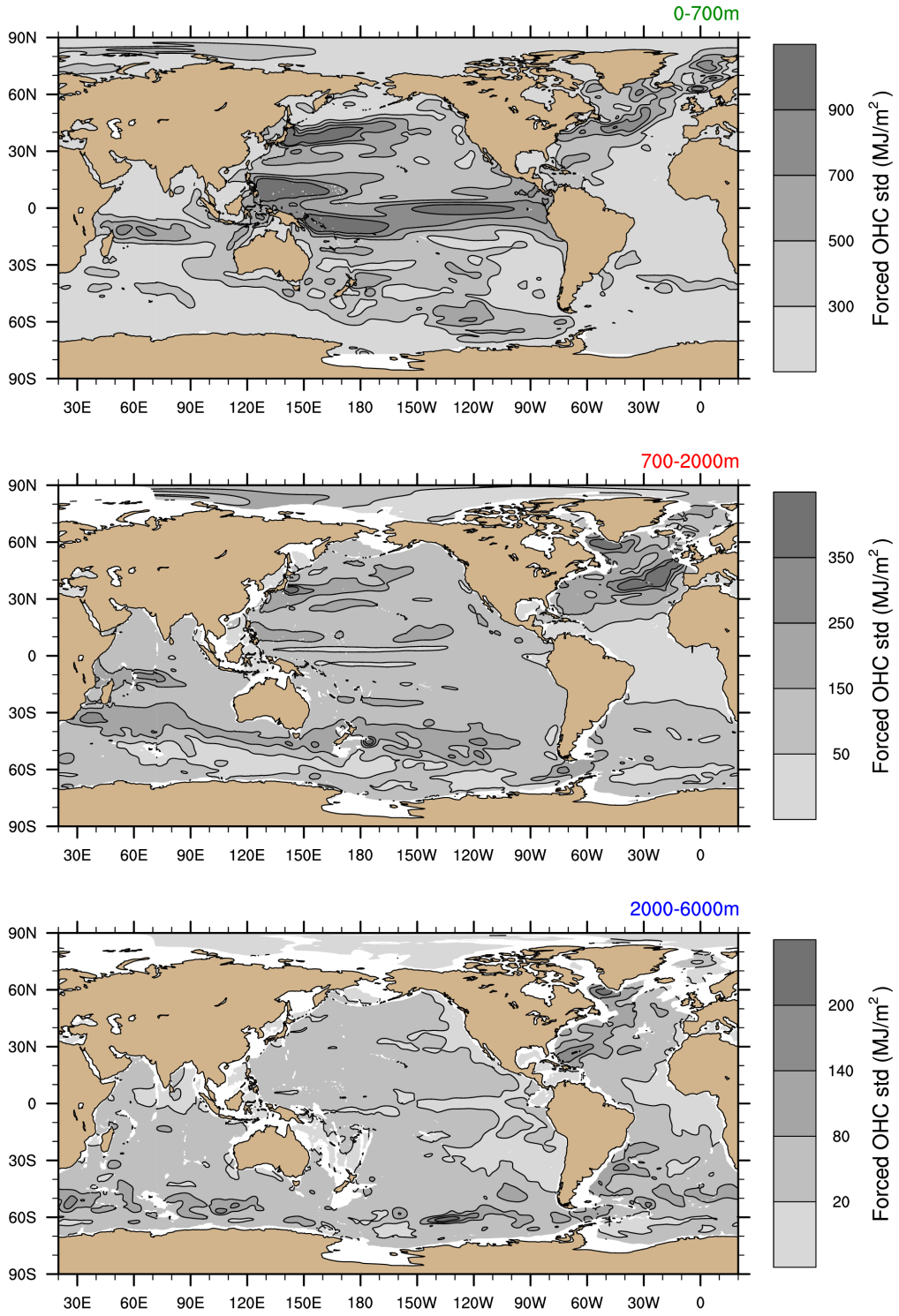

Figure S4. Same as Fig.S3, but for the forced interannual-to-decadal OHC standard deviation.

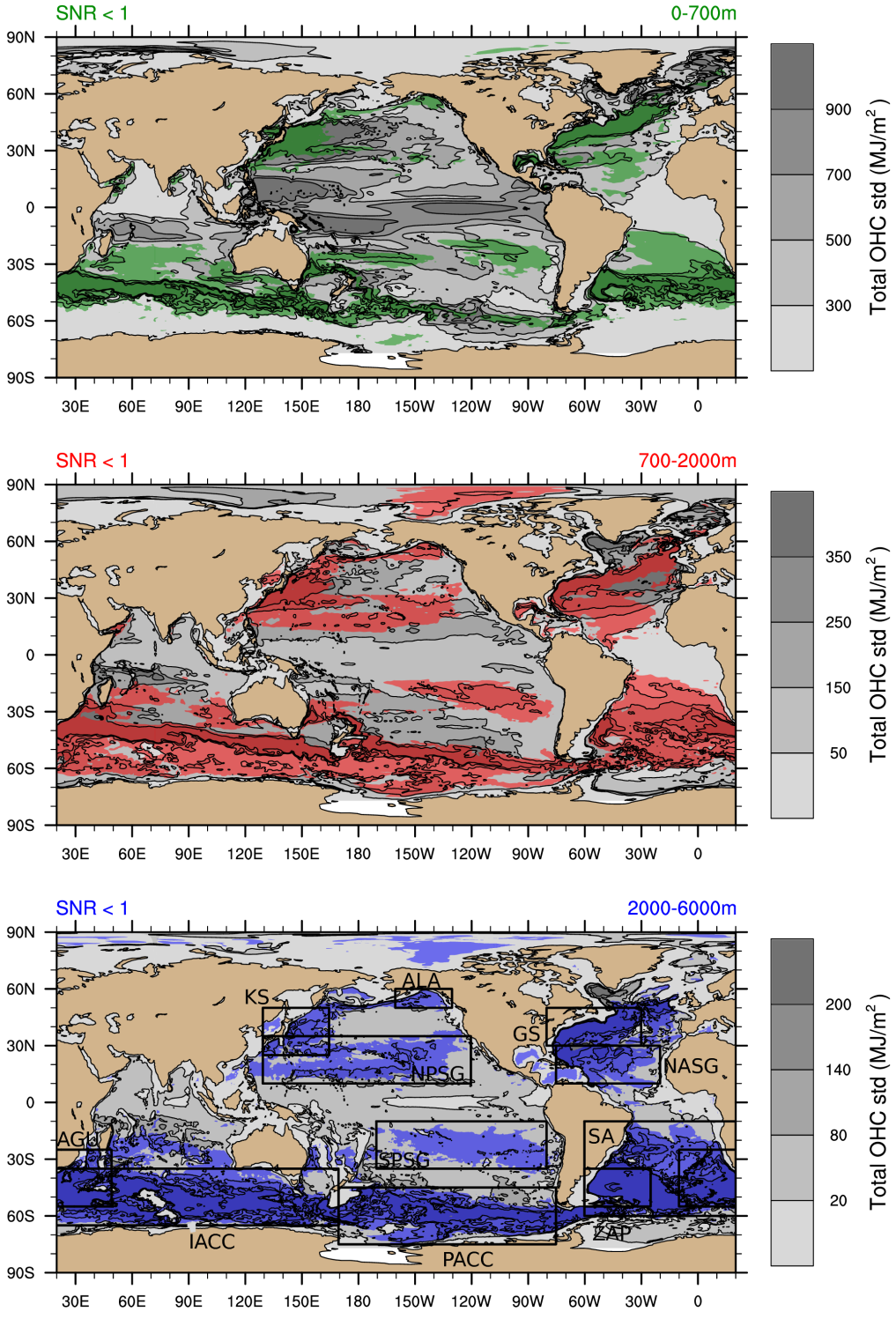

Figure S5. Same as Fig. 1 in the paper for all spatial scales, i.e., with no spatial filtering.